ChemComm

RSC Publishing

COMMUNICATION

Atomic-scale structures and interactions between the guanine quartet and potassium

Cite this: *Chem. Commun.*, 2013, **49**, 7210

Received 3rd May 2013,
Accepted 18th June 2013

DOI: 10.1039/c3cc43302a

www.rsc.org/chemcomm

Wei Xu,*[ab] Qinggang Tan,[a] Miao Yu,[b] Qiang Sun,[a] Huihui Kong,[a] Erik Lægsgaard,[b] Ivan Stensgaard,[b] Jørgen Kjems,[b] Jian-guo Wang,*[c] Chen Wang[d] and Flemming Besenbacher*[b]

The atomic-scale identification of the G_4K_1 structural motif is achieved using an interplay of STM imaging and DFT calculations. Its high stability is found to be caused by the delicate balance between hydrogen bonding and metal–ligand interaction, which is of utmost relevance to model interactions of the G-quadruplex with cations *in vivo*.

Guanine-rich nucleic acid sequences can form a non-canonical four-stranded topology called the G-quadruplex. It is formed by stacked G-quartets stabilized by centrally positioned monovalent Na^+ and K^+ cations.[1] Such an architecture has evolved in nature where it plays several key biological roles in the maintenance of cellular life. A well-studied particular example is the G-quadruplex formed by telomeric sequences at the end of linear chromosomes where they control genomic integrity, chromosomal recombination as well as nucleation points for chromosomal segregation during cell division. Of special interest is that the formation of the G-quadruplex structure can inhibit the activity of telomerase, the cellular enzyme responsible for extending the termini of replicating chromosomes, and hence play a role in maintaining the integrity of the telomere and immortalization of cell.[2] In accordance with this notion cancer cells usually express increased levels of telomerase to maintain the stablility of chromosomes, and the activity of telomerase constitutes an important drug target for current cancer therapy.[3–7] Hence, ligands that can facilitate the formation or stabilize the G-quadruplex structure have been considered as potential anticancer drugs.[8–14]

To rationally design ligands that can effectively bind G-quadruplexes, a fundamental understanding of the interactions between ligands and G-quadruplexes is required. As important cations in cellular environments, potassium ions (K^+) can stabilize the G-quadruplex structure *in vivo* and inhibit the activity of telomerase.[2] In biological systems the G-quadruplexes are found to be mainly stabilized by a combination of hydrogen bonding (HB) and metal–ligand (M–L) interaction. However, the different contributions from the fundamental interactions (*e.g.* HB and M–L interaction) are still under debate. In this communication we employ G-quartet–K as a model system to study the fundamental interactions between the G-quartet and K *in vitro* on a clean and well controlled template, Au(111) surface. Using the interplay of high-resolution Scanning Tunneling Microscopy (STM) imaging and Density Functional Theory (DFT) calculations we reveal the atomic-scale structures of G-quartet–K motifs and quantify the balance between HB and M–L interaction in this model system. We find that G_4K_1 is a very stable structure resulting from the cooperative effect of HB and M–L interaction. Such information is of the utmost significance (i) in the improved modeling of the interactions of G-quadruplexes with K^+ in solution *in vivo*, and (ii) for our basic understanding of the delicate balance of the fundamental forces responsible for keeping the G-quadruplex–K structures stable.

The experiments were performed in an ultra high vacuum (UHV) chamber equipped with a variable-temperature "Aarhus-type" STM from SPECS.[15] After thorough degassing, the G molecules were initially deposited by thermal sublimation at 420 K onto a clean Au(111) substrate held at room temperature (RT), and subsequently the K atoms were deposited onto the G covered surface at RT. The sample was thereafter transferred within the UHV chamber to the STM, where measurements were carried out in a temperature range of 120–150 K. All DFT calculations are performed using the GPAW program.[16,17] In order to accurately describe the hydrogen bonded complexes, optB88-vdw was used to describe the exchange–correlation effects.[17]

Fig. 1a shows the STM topography image of the metallosupramolecular G-quartet network motif corresponding to a low K dose. As previously demonstrated, the formation of G-quartet networks is predominately steered by inter- and intra-quartet hydrogen bonds, and the G molecules, which are lying flat on the surface, are imaged as triangular protrusions.[18–22] As directly revealed in Fig. 1a, the K deposition results in the appearance of a central protrusion within

[a] *College of Materials Science and Engineering, Key Laboratory for Advanced Civil Engineering Materials (Ministry of Education), Tongji University, Caoan Road 4800, Shanghai 201804, P. R. China. E-mail: xuwei@tongji.edu.cn*
[b] *Interdisciplinary Nanoscience Center (iNANO), Center for DNA Nanotechnology (CDNA), Department of Physics and Astronomy, and Department of Molecular Biology, Aarhus University, DK 8000 Aarhus C, Denmark. E-mail: fbe@inano.au.dk*
[c] *Institute of Industrial Catalysis, College of Chemical Engineering and Materials Science, Zhejiang University of Technology, Hangzhou, 310032, P. R. China. E-mail: jgw@zjut.edu.cn*
[d] *National Center for Nanoscience and Technology, Beijing 100190, P. R. China*

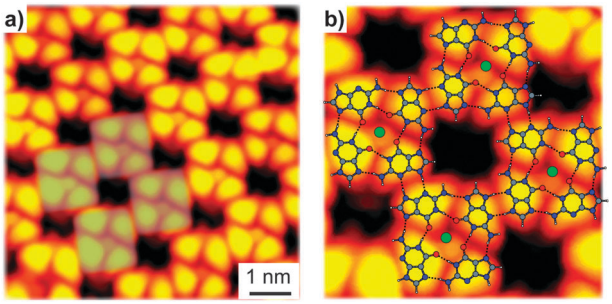

Fig. 1 STM topography image of the metallosupramolecular G-quartet network resulting from the low K dose. (a) High-resolution STM image of the G_4K_1 network. (b) The DFT proposed model of the G_4K_1 network is superimposed on the close-up STM image.

each G-quartet motif, which is suggestive of only one K atom being bound in each G-quartet (*i.e.* G_4K_1). Since the G-quartet network is still maintained after the K deposition the hydrogen-bonded G-quartet motifs are assumed not to be much affected by the incorporation of K atoms. In Fig. 1b the theoretical model from the DFT calculations is superimposed on the enlarged STM image cut out from the region highlighted in Fig. 1a. The K atom is found from the STM images to be located in the center of the G-quartet and the distances between the K atom and the four O atoms of the G molecules are all 2.60 Å, and the K atom is 1.04 Å higher than the G-quartet plane. As can be identified from the resulting model there are two kinds of interactions (i) hydrogen bonding (N–H···O, N–H···N) and (ii) metal–ligand bonding (K–O) to stabilize the G_4K_1 network. Note that the G_4K_1 network can withstand higher temperatures of 470–490 K than the G-quartet network (*ca.* 410 K).

The fundamental G_4K_1 motif is very relevant to the reported G-quadruplex structures found in biology.[23,24] Numerous studies have dealt with the structure, conformational diversity and dynamics of human telomeric G-quadruplexes using various techniques such as NMR spectroscopy, single-molecule fluorescence resonance energy transfer, electrospray mass spectrometry, single-crystal X-ray diffraction.[25–29] Our combined STM and DFT study may help to gain further real-space atomic-scale insights into the biologically relevant G–K motif by reducing the complexity of the system from 3D to 2D.

To further unravel the nature of the G_4K_1 motif, Bader charge analysis is performed, which shows that in the G_4K_1 motif the K atom donates 0.87 electrons to G molecules, thus the K atom exhibits cationic characteristics after interacting with G molecules. So we identify that the interaction between the K atom and the G molecules should be mainly attributed to ionic interaction.[30,31] Moreover, an analysis of charge density difference maps and integrated charge density differences over the *x* and *y* dimensions was performed for the G_4 and G_4K_1 motifs in order to explore the role of K in the stabilization of G-quartet as demonstrated in Fig. 2. In the absence of K atoms (*cf.* Fig. 2a), the charge transfer between the donor and acceptor groups is responsible for the strong HB, and the charges are mainly accumulated on the O atoms of G molecules (*cf.* Fig. 2c and d left panels). However, when the K atom is bound to the center of the G-quartet (*cf.* Fig. 2b), it not only induces more charge accumulation on the O atoms but also screens the electrostatic repulsion between these negatively charged O atoms (*cf.* Fig. 2c, middle and right panels). The induced charge density

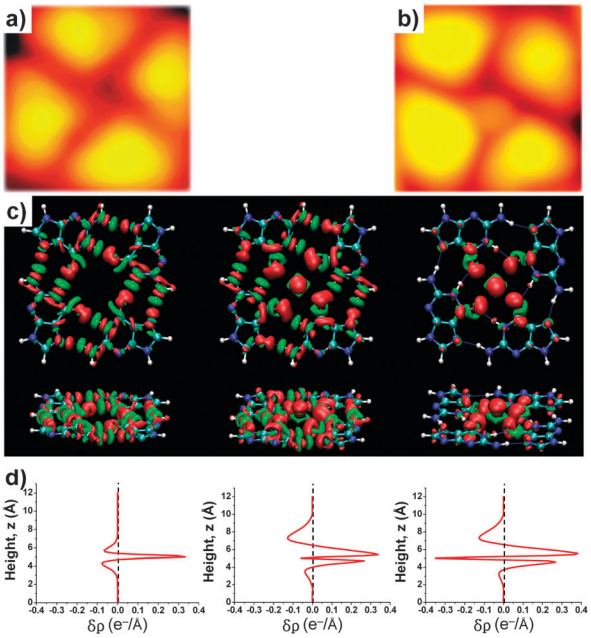

Fig. 2 Charge density difference maps of the G_4 and G_4K_1 clusters. (a) The enlarged G_4 motif. (b) The enlarged G_4K_1 motif. (c) The top and side views of charge density difference maps of G_4 (left panel) and G_4K_1 motifs (middle panel: the four G molecules and the K atom are considered to be five individual species; right panel: the four G molecules are considered to be a whole and the K atom is considered to be another individual species). (d) The integrated charge density differences over the *x* and *y* dimensions.

plots (Fig. 2d) illustrate the distribution of electron density between the K atoms and the four O atoms in G_4 and G_4K_1. The plots show the induced charge density integrated over the lateral dimensions and since the K atoms reside at higher position than the G molecules the downward electron charge rearrangement evidences charge transfer from K to G. This electron charge rearrangement is enhanced with the K atom (Fig. 2d middle and right panels, respectively), which indicates an electrostatic origin of the enhanced G-quartet stability with the embedded K atoms.

The DFT calculated formation energies of the G-quartet network, the isolated G quartets and their constituent dimers and trimers with and without one K atom are plotted in Fig. 3, upper panel. As discussed in our previous study,[18] the formation energy of the G dimer, trimer and quartet structures scales superlinearly with the number of hydrogen bonds between the guanine molecules (*cf.* Fig. 3 upper panel, blue triangles are above the blue dashed line) due to the resonance-assisted hydrogen bonding (RAHB). The addition of the K atom further enhances the RAHB of these structures as evidenced by the larger differential formation energy of guanine in G_nK_1 than that in G_n. The formation energy difference between G_nK_1 and G_n (n = 2–4) depends strongly on the number of G in the structures, increasing from 1.07 eV, 1.48 eV, 1.73 eV to 1.85 eV from the isolated dimer, trimer, and quartet to the quartet in the networks. We can thus conclude that the stability of G structures by the addition of K increases with increasing the number of metal–ligand bonds. The induced charge density plots for the G_n, G_nK_1 (n = 2–4) clusters and the networks with and without K are depicted in Fig. 3, lower panel. Comparing G_nK_1 with G_n (n = 2–4) it is seen that the intramolecular charge perturbation ascribed to hydrogen

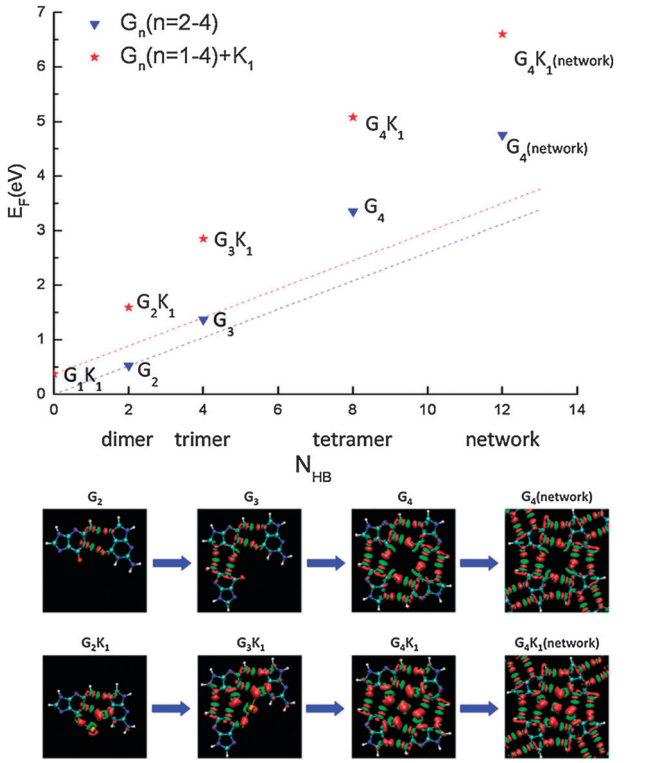

Fig. 3 The calculated formation energies of the G-quartet network, the isolated G quartet and their constituent dimer and trimer with and without one K atom are plotted (upper panel). The induced charge density plots for the G_n and G_nK_1 (n = 2–4) clusters and the networks with and without one K atom are shown (lower panel). The blue dashed line is defined as the straight line from the origin through the G_2 data point. The red dashed line is parallel to the blue dashed line, but starts at the G_1K_1 data point.

bonding becomes more pronounced by increasing the number of G molecules, thus nicely illustrating the enhancement of the RAHB effect (*cf.* Fig. 3 upper panel: red stars are above the red dashed line). Compared with and without K, Bader charge analysis reveals that the oxygen atoms gain more electron charge (about 0.05 electrons per O atom) in the presence of K. This is particularly clear for G_2K_1 and G_3K_1 but carries through to the G-quartet cluster as discussed above. From the G-quartet cluster to the network, although the charge of the oxygen atom does not change much, the nitrogen atom involved in the inter-quartet hydrogen bonds (N–H···N) gains more electron charge (about 0.10 and 0.15 electrons per N atom) in G_4 and G_4K_1 networks than that in G_4 and G_4K_1 clusters, respectively. Taken together, the plots suggest that the extraordinary stability of the K-promoted G-quartet motif is caused not only by the hydrogen bonding (with RAHB effect) but also by the M–L interaction.

In conclusion, using the interplay between high-resolution STM imaging and DFT calculations we have revealed the real-space atomic-scale structure of the G_4K_1 motif, and quantitatively demonstrated that the stability of the G_4K_1 structure is due to the delicate balance between hydrogen bonding and metal–ligand interaction, which is of utmost relevance to model interactions of the G-quadruplex with cations *in vivo*. The present results provide fundamental insights into the structural aspects of the interaction of the G-quartet motif with K, and further studies on the investigation of interactions between other biologically relevant metallic atoms or small-molecule ligands and G-quartets will be carried out to get a deeper understanding of the structural and energetic aspects of how the G-quadruplex could be stabilized by the ligands. Since the G-quadruplex structure inhibits the telomerase enzyme which controls the replications of chromosomes, the results may be of relevance for the further development of anti-cancer drug design.

The authors acknowledge financial support from the Danish Ministry for Science, Technology and Innovation, Danish Research Councils, Danish National Research Foundation, The Carlsberg Foundation, Danish Center for Scientific Computing, National Natural Science Foundation of China (No. 21103128, 21176221, 21136001), Shanghai "Pujiang" program (11PJ1409700), Shanghai "Shu Guang" project (11SG25), National Basic Research Program of China (973 Program) (2013CB733501). Bjørk Hammer is greatly acknowledged for fruitful discussion and Zheshen Li for providing the K source.

Notes and references

1 M. Gellert, M. N. Lipsett and D. R. Davies, *Proc. Natl. Acad. Sci. U. S. A.*, 1962, **48**, 2013.
2 A. M. Zahler, J. R. Williamson, T. R. Cech and D. M. Prescott, *Nature*, 1991, **350**, 718.
3 C. Philippi, B. Loretz, U. F. Schaefer and C. M. Lehr, *J. Controlled Release*, 2010, **146**, 228.
4 S. Neidle and G. Parkinson, *Nat. Rev. Drug Discovery*, 2002, **1**, 383.
5 J. W. Shay and W. E. Wrigh, *Nat. Rev. Drug Discovery*, 2006, **5**, 577.
6 B. S. Herbert, A. E. Pitts, S. I. Baker, S. E. Hamilton, W. E. Wright, J. W. Shay and D. R. Corey, *Proc. Natl. Acad. Sci. U. S. A.*, 1999, **96**, 14276.
7 J. W. Shay and W. E. Wrigh, *Cancer Cell*, 2002, **2**, 257.
8 S. Neidle and M. A. Read, *Biopolymers*, 2000, **56**, 195.
9 H. Han and L. H. Hurley, *Trends Pharmacol. Sci.*, 2000, **21**, 136.
10 L. Oganesian and T. M. Bryan, *Bioessays*, 2007, **29**, 155.
11 S. Neidle, *FEBS J.*, 2010, **277**, 118.
12 A. Bugaut, K. Jantos, J. L. Wietor, R. Rodriguez, J. K. M. Sanders and S. Balasubramanian, *Angew. Chem., Int. Ed.*, 2008, **47**, 2677.
13 S. Balasubramanian, L. H. Hurley and S. Neidle, *Nat. Rev. Drug Discovery*, 2011, **10**, 261.
14 J. S. Hudson, S. C. Brooks and D. E. Graves, *Biochemistry*, 2009, **48**, 4440.
15 E. Lægsgaard, L. Österlund, P. Thostrup, P. B. Rasmussen, I. Stensgaard and F. Besenbacher, *Rev. Sci. Instrum.*, 2001, **72**, 3537.
16 J. P. Perdew and Y. Wang, *Phys. Rev. B*, 1992, **45**, 13244.
17 S. R. Bahn and K. W. Jacobsen, *Comput. Sci. Eng.*, 2002, **4**, 56.
18 R. Otero, M. Schöck, L. M. Molina, E. Lægsgaard, I. Stensgaard, B. Hammer and F. Besenbacher, *Angew. Chem., Int. Ed.*, 2005, **44**, 2270.
19 W. Xu, R. E. A. Kelly, H. Gersen, E. Lægsgaard, I. Stensgaard, L. N. Kantorovich and F. Besenbacher, *Small*, 2009, **5**, 1952.
20 R. Otero, W. Xu, M. Lukas, R. E. A. Kelly, E. Lægsgaard, I. Stensgaard, J. Kjems, L. N. Kantorovich and F. Besenbacher, *Angew. Chem., Int. Ed.*, 2008, **47**, 9673.
21 W. Xu, J. Wang, M. F. Jacobsen, M. Mura, M. Yu, R. E. A. Kelly, Q. Meng, E. Lægsgaard, I. Stensgaard, T. R. Linderoth, J. Kjems, L. N. Kantorovich, K. V. Gothelf and F. Besenbacher, *Angew. Chem., Int. Ed.*, 2010, **49**, 9373.
22 W. Xu, J. Wang, M. Yu, E. Lægsgaard, I. Stensgaard, T. R. Linderoth, B. Hammer, C. Wang and F. Besenbacher, *J. Am. Chem. Soc.*, 2010, **132**, 15927.
23 C. Detellier and P. Laszlor, *J. Am. Chem. Soc.*, 1980, **102**, 1135.
24 S. L. Forman, J. C. Fettinger, S. Pieraccini, G. Gottarelli and J. T. Davis, *J. Am. Chem. Soc.*, 2000, **122**, 4060.
25 W. Eimer and T. Dorfmüller, *J. Phys. Chem.*, 1992, **96**, 6790.
26 A. A. Lipanov, J. Quintana and R. E. Dickerson, *J. Biomol. Struct. Dyn.*, 1990, **8**, 483.
27 K. J. Koch, T. Aggerholm, S. C. Nanita and R. G. Cooks, *J. Mass Spectrom.*, 2002, **37**, 676.
28 G. Wu and A. Wong, *Chem. Commun.*, 2001, 2658.
29 L. M. Ying, J. J. Green, H. T. Li, D. Klenerman and S. Balasubramanian, *Proc. Natl. Acad. Sci. U. S. A.*, 2003, **100**, 14629.
30 Y. Kim, S. Yau and K. Itaya, *J. Am. Chem. Soc.*, 1996, **118**, 393.
31 N. Abdurakhmanova, A. Floris, T. Tseng, A. Comisso, S. Stepanow, A. De Vita and K. Kern, *Nat. Commun.*, 2012, **3**, 940.

